Research Article

Nano Ag-Doped In$_2$O$_3$ Thick Film: A Low-Temperature H$_2$S Gas Sensor

D. N. Chavan,[1] G. E. Patil,[2] D. D. Kajale,[2] V. B. Gaikwad,[3] P. K. Khanna,[4] and G. H. Jain[2]

[1] *Department of Chemistry, Arts Commerce and Science College, Lasalgaon 422 306, India*
[2] *Materials Research Lab., Arts, Commerce and Science College, Nandgaon 423 106, India*
[3] *Materials Research Lab., K.T.H.M. College, Nashik 422 005, India*
[4] *Applied Chemistry and Nanoscience DIAT, Govt. of India, Girinagar Pune 411 025, India*

Correspondence should be addressed to G. H. Jain, gotanjain@rediffmail.com

Thick films of AR grade In$_2$O$_3$ were prepared by standard screen-printing technique. The gas sensing performances of thick films were tested for various gases. It showed maximum sensitivity to ethanol vapour at 350°C for 80 ppm concentration. To improve the sensitivity and selectivity of the film towards a particular gas, In$_2$O$_3$ sensors were surface-modified by dipping them in a solution of 2% nanosilver for different intervals of time. Obtained results indicated that spherical nano-Ag grains are highly dispersed on the surface of In$_2$O$_3$sensor. The surface area of the nano-Ag/ In$_2$O$_3$ sensor is several times larger than that of pure In$_2$O$_3$ sensor. In comparison with pure In$_2$O$_3$ sensor, all of the nano-Ag-doped sensors showed better sensing performance in respect of response, selectivity, and optimum operating temperature. The surface-modified (30 min) In$_2$O$_3$ sensor showed larger sensitivity to H$_2$S gas (10 ppm) at 100°C. Nano silver on the surface of the film shifts the reactivity of film from ethanol vapour to H$_2$S gas. A systematic study of gas sensing performance of the sensor indicates the key role played by the nano silver species on the surface. The sensitivity, selectivity, response, and recovery time of the sensor were measured and presented.

1. Introduction

Hydrogen Sulphide (H$_2$S) is a colourless, toxic, flammable, and malodorous gas as sources from gasoline, natural gases, city sewage, volcanic gases, and hot springs with smells like rotten eggs. It can also be produced from bacterial breakdown of organic matter or wastes produced by humans and animals. Other sources are craft paper mills, tanneries, and petroleum refineries. H$_2$S gas is badly harmful to human body and the environment. According to the safety standards established by American Conference Government Industrial Hygienists, the threshold limit value (TLV) defined for H$_2$S is 10 ppm. Meanwhile the type of oil and natural gas is correlative with the concentration of H$_2$S. The oil and natural gases mines can be found depending on the concentration of H$_2$S. Therefore, the detection and monitoring of H$_2$S are of high importance for both resource exploitation and human health. In the recent researches, a number of semiconductor sensors have been found to be sensitive to H$_2$S including WO$_3$, In$_2$O$_3$, ZnO, and a few perovskite-type materials [1–9].

In general, metal oxide materials are rarely used as a single phase for sensors. And their gas sensing characteristics are usually well modified by adding a small amount of catalysts. Platinum and Palladium are well known active catalysts, which enhance the sensitivity against reducing gases [10]. Gold (Au), Silver (Ag) are also utilized to enhance the sensitivity of oxide materials [11]. It is believed that the catalysts promote chemisorptions process and thus increase the density of chemisorbed oxygen species, which are reaction centres for reducing gas molecules. The addition of second component in metal oxide semiconductor gas sensor either as bulk doping or as surface modification is one of the successful methods to optimize and improve the properties of gas sensors [12–17].

Semiconductor metal oxide-based gas sensors have been a subject of extensive research because of their use in detecting several toxic inflammable and odourless gases [18–23].

The sensing properties are based on the reaction between semiconducting metal oxides and gases in the atmosphere. The gas sensing mechanism involves the redox reaction at the surface, leading to the changes in the depletion layer of the grains that in turn changes the electrical resistance [24–28]. There are many possible reactions for the changes in electrical resistance; the most common reaction that leads to changes in the conductance is the adsorption of gases on the semiconducting surface. With the adsorption being a surface effect, great emphasis has been placed in the research towards the study of nanosized materials. In nanosized materials, a large fraction of the atoms is present at the surface, and hence, the surface properties become dominant. Hence, for the application of semiconducting metal oxide, as a sensing layer material of chemical gas sensors, nanosized particles are desirable. Indium oxide offers new advantages in designing metal oxide-based gas sensors, linked with an essential difference in electrophysical and chemical properties between SnO_2 and In_2O_3. As a gassensing material, In_2O_3 has been extensively applied to detect O_3, NO_2 and CO [29–31]. In_2O_3 is known as to be an n-type semiconductor in its nonstoichiometric form, due to oxygen vacancy doping and has been extensively studied as a conductivity-based chemical sensor [32].

Due to advantages such as small size, low cost, simple operation, and good reversibility, the semiconductor sensors have become the most promising devices among the solid-state chemical sensors. Hence, the metal oxide gas sensing materials are widely investigated. Many semiconductor oxides such as SnO_2, ZnO, Fe_2O_3, In_2O_3, WO_3, and CuO have been explored to be detecting the polluting toxic and inflammable gases, such as CO, CO_2, NO_x, H_2S, and ethanol [33–37].

In the present study, the nano-Ag is used for surface modification of In_2O_3 thick film. It has been described that the nano-Ag particles on the surface of In_2O_3 films by dipping technique improves the surface adsorption capability. As a result of the numerous interfaces between the nano-grains that interact with gas molecules can effectively improve the diffusion properties, while greatly increasing the gas sensitivity of the materials [38–40]. The nano-Ag used in the present work was prepared as described in the literature [41].

In this work, In_2O_3 thick films were prepared and deposited by screen printing on to glass substrates. The films surface were modified by dipping them into the solution of nano-Ag. The sensing performance of the films were tested by static gas sensing system for different gases such as H_2S, CO, CO_2, H_2, LPG, NH_3, Cl_2, O_2, and ethanol vapour.

2. Experimental

The AR grade powder of In_2O_3 was calcined at $1000°C$ for 6 h. Then In_2O_3 powder was milled for 2 hrs using planetary ball mill to obtain fine-grained powder. The thixotropic paste was formulated by mixing the fine powder of In_2O_3 with a solution of ethyl cellulose (a temporary binder) in a mixture of organic solvents such as butyl cellulose, butyl carbitol acetate, and terpineol. The weight ratio of the inorganic to organic part was kept at 75 : 25 in formulating the paste. This paste was screen-printed on a glass substrate in a desired pattern [42–44]. The sensors were fired at $550°C$ for 30 min. Silver contacts are made for electrical measurements. The preparation of nano-Ag colloidal solution was explained elsewhere [41]. The pure In_2O_3 sensors were surface-modified by dipping them into 2% nanosilver solution for different intervals of time: 5, 10, 15, 20, 30, and 45 min [45]. The oxidation state of nano-Ag in colloidal state is zero. These sensors were dried under IR lamp at $80°C$ for 1 h and followed by firing at $550°C$ for 30 minutes. During firing process nano-$Ag°$ was converted into Ag_2O (with oxidation state +1). The thickness of the sensors was measured by using the Taylor-Hobson (Talystep, UK) system and was observed in the range from 60 to $65 \mu m$. The reproducibility of the sensors' thickness was achieved by maintaining the proper rheology and thixotropy of the paste.

The sensing performance of the sensors was examined using a "static gas sensing system." There were electrical feeds through the base plate. The heater was fixed on the base plate to heat the sample under test up to required operating temperatures. The current passing through the heating element was monitored using a relay operated with an electronic circuit with adjustable on-off time intervals. A Cr-Al thermocouple was used to sense the operating temperature of the sensor. The output of the thermocouple was connected to a digital temperature indicator. A gas inlet valve was fitted at one of the ports of the base plate. The required gas concentration inside the static system was achieved by injecting a known volume of a test gas using a gas-injecting syringe. A constant voltage was applied to the sensor, and the current was measured by a digital Pico ammeter. The air was allowed to pass into the glass chamber after every gas exposure cycle.

3. Results

The purity and crystallinity of the calcined powder structure were examined using X-ray diffractogram (XRD) with CuKα radiation (wavelength 1.5418 Å). The average grain size was calculated according to Debye-Scherrer's equation; it was observed to be 51 nm. Figure 1, depicts that the XRD patterns are indexed with pure In_2O_3 with cubic structure. The observed peaks in figure are matched well with (JCPDS Card no. 01-071-2194) reported data of In_2O_3 [46]. Figure 2, shows the micrographs of pure In_2O_3 and nano-Ag surface-modified In_2O_3 sensors. The comparison of these micrographs shows the interesting changes in morphology. Scanning electron microscopic (SEM) studies were carried out by using JEOL JSM 6360 (LA) Japan. Figure 2(a) depicts the SEM image of pure In_2O_3 sensor fired at $550°C$. The sensor consists of voids and a wide range of grains with size distribution ranging from $0.25 \mu m$ to $0.5 \mu m$, distributed nonuniformly. Figure 2(b) represents the SEM image of nano-Ag surface-modified In_2O_3 (30 min) sensor fired at $550°C$. It shows a number of small particles distributed uniformly between the larger grains around the In_2O_3, which may be attributed to the presence of nano-Ag. The grain

TABLE 1: Quantitative elemental analysis of pure and nano-Ag surface modified In_2O_3 sensors.

Film	In (wt%)	O (wt%)	Ag (wt%)
Pure In_2O_3	41.33	58.67	—
Nano-Ag Surface Modified			
Dipping time: 5 min	37.90	61.93	0.17
Dipping time: 10 min	40	59.69	0.22
Dipping time: 15 min	39.34	60.43	0.23
Dipping time: 20 min	42.70	57.05	0.25
Dipping time: 30 min	44.59	55.03	0.38
Dipping time: 45 min	39.67	59.9	0.43

FIGURE 1: X-ray diffractogram of pure In_2O_3.

size range was observed to be from $0.05\,\mu$m to $0.5\,\mu$m. The presence of nano-Ag particles on the surface of the sensor alters the adsorption-desorption ability of the sensor. The altered surface morphology of the sensor shifts the affinity and reactivity of sensor towards the H_2S gas. EDAX analysis of nanosilver surface-modified sensor shows the presence of nanosilver, and the appearance from the sensor indicates that the nanosilver particles are present at the surface of the In_2O_3 sensor.

The quantitative elemental analysis of the pure and nano-Ag surface-modified In_2O_3 sensors was carried out by using an energy dispersive spectrophotometer (EDS) JEOL-JED-2300 LA Japan. The constituent elements such as In, O, and Ag associated with various sensors are presented in Table 1. It is clear from Table 1 that the weight percentage of silver is increased with dipping time and reached to a maximum. The sensor with the dipping time of 30 min as we observed to be more oxygen deficient (55.03 wt.%). This oxygen deficiency may make the sample possible to adsorb a large amount of oxygen species.

Figure 3 shows the I-V characteristics of pure In2O3 sensor at room temperature. I-V characteristics are observed to be symmetrical in nature, indicating the ohmic nature of silver contact.

Figure 4 shows the dependence of electrical conductivity of pure In_2O_3 and surface modified by nano-Ag In_2O_3 sensors in air ambience. The electrical conductivity of these sensors goes on increasing with increase in temperature, indicating negative temperature coefficient (NTC) of resistance. This shows the semiconducting nature of the sensors.

Figure 5 shows the variation in the gas response of ethanol vapour (80 ppm) with operating temperatures ranging from $50°$C to $450°$C. It is noted from the graph that response increases with increasing temperature, attains a maximum at $350°$C, and decreases with further increase in operating temperature.

Selectivity is defined as the ability of sensor to respond to a certain gas in the presence of other gases. Selectivity is another important parameter of a gas sensor. The sensor must have rather high selectivity for its application. Pure In_2O_3 sensor is examined for different gases at different operating temperatures, and the results are shown in Figure 6. The bar diagram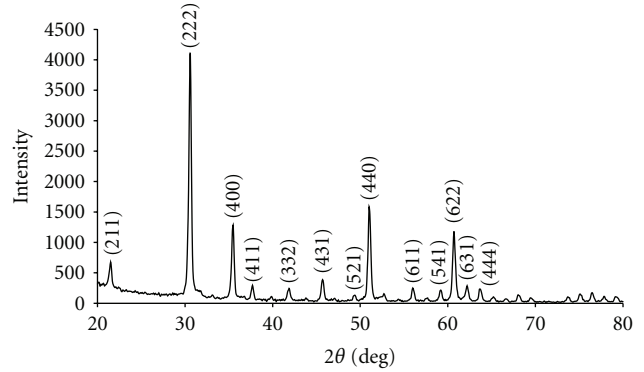 indicatves selectivity of pure In_2O_3 sensor at $350°$C to ethanol vapour against the other gases. The sensor is the most selective to ethanol vapour against the other gases.

Response time and recovery time are the basic parameters of the gas sensors. Which is defined as the time taken for the sensor to attain 90% of maximum change in resistance on exposure to gas is the response time. The time taken by the sensor to get back 90% of the original resistance is the recovery time [47]. The 90% response time and recovery time were attained within 6 s and 60 s, respectively. The very short response time is the important features of the nano-Ag surface-modified (30 min.) In_2O_3 sensor. The large recovery time would be due to lower operating temperature. At lower temperature O_2^- species is more prominently adsorbed on the surface, and thus it is less reactive as compared to other species of oxygen, O^- and O^{--}.

The enhanced response of nano-Ag surface-modified sensors can be attributed to two factors. First the higher specific surface areas of the nano-Ag doped sensors can lead to increase in active surface area for gas sensing. Secondly, the nano-Ag dopant, as a catalyst, enhances the adsorption of gas molecules and accelerates the electron exchange between the sensor and test gas [48]. The two factors together contribute to the improvement of gas sensing properties of nano-Ag surface-modified In_2O_3 sensors. Furthermore, the maximum response is observed for nano-Ag surface-modified (30 min) In_2O_3 sensor, perhaps due to the largest amount of active reaction sites formed on the surface of In_2O_3 sensor by the random dispersion of nano-Ag [49].

4. Discussion

Since long it has been known that adsorption of reducing gas molecules results in decrease in electrical resistance of oxide material [50]. The In_2O_3 materials are characteristically n-type semiconductor due to nonstoichiometry associated with oxygen vacancy and/or metal excess which acts as donor states thus providing conduction electrons. However, the overall surface resistance of such films is generally influenced by chemisorptions (chemical adsorption) of oxygen from air on the surface and at the grain boundaries. The chemisorbed oxygen traps conduction electrons and remains as negatively
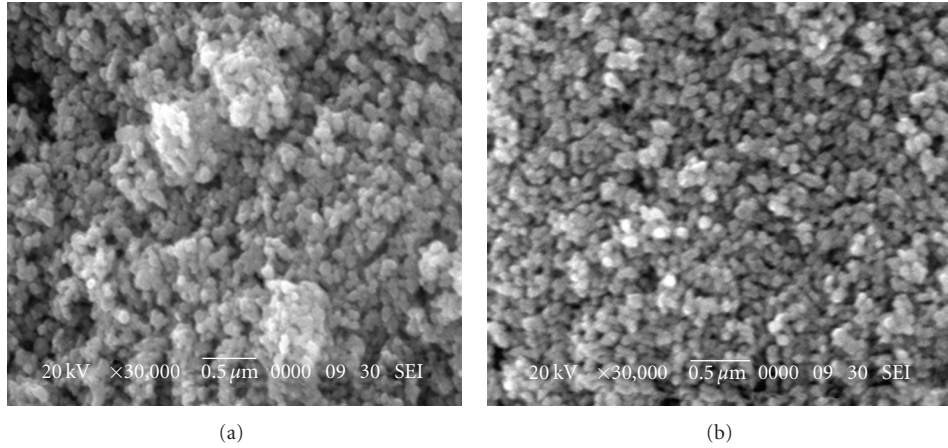
(a)

(b)

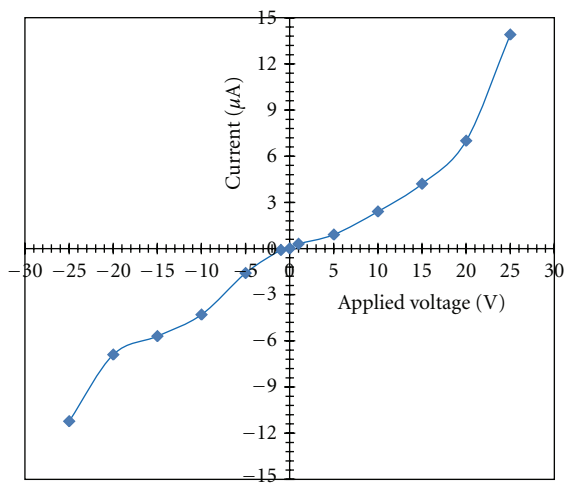FIGURE 2: SEM images of (a) pure In$_2$O$_3$ and (b) nano-Ag surface-modified In$_2$O$_3$ (30 min) sensors.

FIGURE 3: I-V characteristics of pure In$_2$O$_3$ sensor.

Pure   5 min
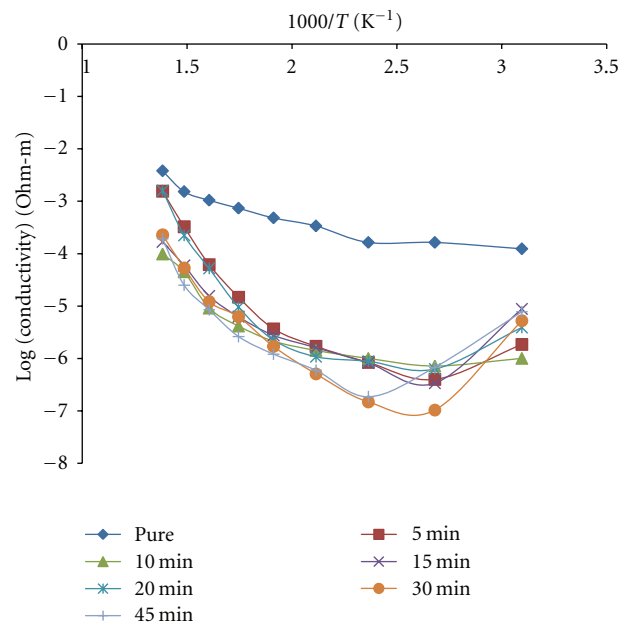10 min   15 min
20 min   30 min
45 min

FIGURE 4: Variation of electrical conductivity with temperature.

charged species (O$_2{}^-$, O$^-$, or O^{2-} depending on temperature) on the surface [51]. The process results in an increase of surface resistance. In presence of reducing gases the trapped electrons are released due to the reaction between the gas molecules and negatively charged chemisorbed oxygen species resulting in decreasing in resistance of the materials. When the gas is removed from the sensor environment, the resistance again increases and the material recovered to original resistance.

Figure 7 shows the variation in the gas response of pure and nano-Ag surface-modified In$_2$O$_3$ sensors to H$_2$S gas (10 ppm) with operating temperature ranging from 50°C to 400°C. The H$_2$S gas response of pure In$_2$O$_3$ sensor fired at 550°C was 0.6 at 100°C while that of nano-Ag surface-modified (30 min) In$_2$O$_3$ sensor was 40010 at the same operating temperature. Therefore, the nano-Ag surface-modified of In$_2$O$_3$ sensors was observed to be excellent for H$_2$S gas sensing than the pure In$_2$O$_3$ sensor.

The nano-Ag surface-modified (30 min) In$_2$O$_3$ sensor showed maximum gas response to H$_2$S gas. The amount of
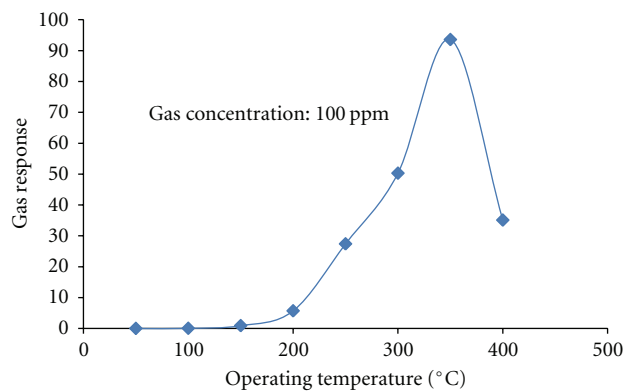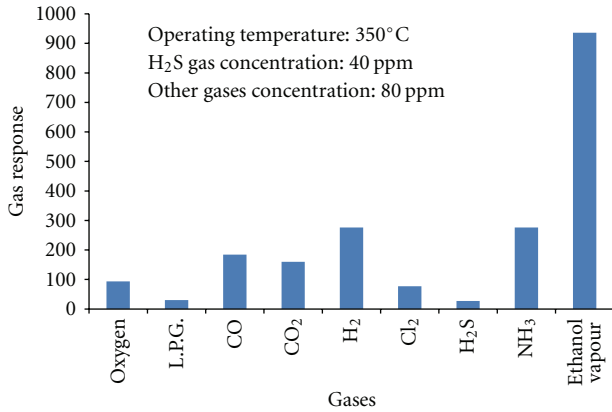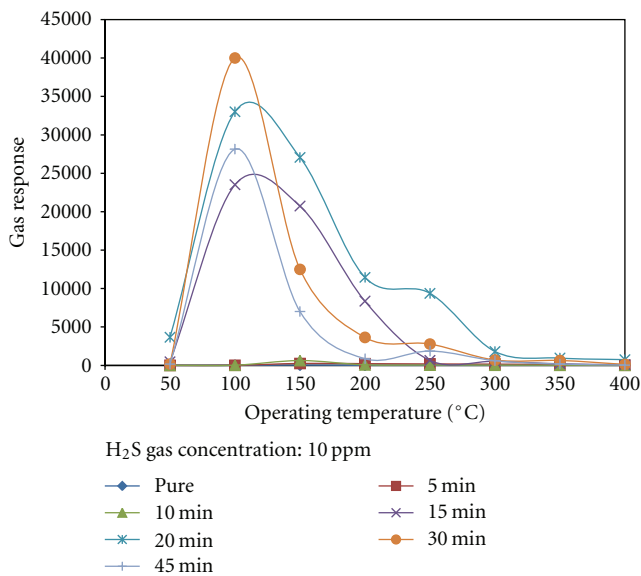

FIGURE 5: Variations of ethanol vapour response of pure In$_2$O$_3$ sensor with operating temperature.

FIGURE 6: Selectivity of pure In_2O_3 sensor.

FIGURE 7: Variation of H_2S gas response with operating temperature.

nano-Ag incorporated onto the In_2O_3 sensor surface would be optimum to cover the surface uniformly, leading to the enhanced adsorption mechanism:

$$Ag_2O + H_2S \longrightarrow Ag_2S + H_2O \uparrow \qquad (1)$$
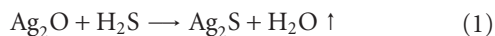
The gas response to H_2S gas goes on increasing with increasing the amount of nano-Ag up to a certain limit, attains maximum gas response, and decreases with increasing the amount of nano-Ag. The largest gas response in case of the sample (30 min) may be because of more available sites (misfits). The surface of nano-Ag misfit regions enhances the oxygen adsorption on the surface. Thus the number of oxygen species adsorbed on the activated surface would be larger. The larger the number of oxygen species adsorbed, the faster the oxidation of H_2S gas would be. The pure In_2O_3 sensor showed the highest response to ethanol vapour, while nano-Ag surface-modified sensor showed it to H_2S gas. The alteration in nature of gas sensing response from ethanol

vapour to H_2S gas for the nano-Ag surface modified In_2O_3 sensor could be largely due to possibility of formation of silver sulphide more easily than formation of silver oxide. This would increase the conductance of the film crucially, enhancing gas response. The abrupt decrease of response for the sensors doped with more amount of Ag is probably due to the reduction of active sites correlated with the agglomeration of Ag grains. At higher concentrations, the nano-Ag would mask the entire base material and would resist the gas to reach to the surface active sites, so gas response would decrease further [52].

It is well known that the gas sensitivity is greatly influenced by the operating temperature and the amounts of additives. In order to determine the optimum operating temperature and additive amount, the gas responses of nano-Ag/In_2O_3 sensors with different nano-Ag content to 10 ppm H_2S gas were measured at different operating temperatures. The gas response of pure In_2O_3 sensor to H_2S gas was also measured for comparison. The results are shown in Figure 8. It can be seen obviously from Figure 8 that the pure In_2O_3 sensor has a poor response to H_2S gas, while the nano-Ag surface-modified sensors with different amounts of Ag; all exhibit much higher gas responses than the pure one. Among the entire nano-Ag surface-modified In_2O_3 sensors, the one with dipping time 30 min (0.38 wt.%) shows the largest gas response to H_2S gas, whilst the gas sensing property change trend is similar to the specific surface area change trend of the samples. Additionally, the gas responses of the sensors to H_2S gas are also affected by the operating temperature. The operating temperature of all the nano-Ag surface-modified sensors is lower than that of the reported H_2S gas sensors [48, 53, 54]. The lower operating temperature could lead to lower energy consumption, while it is one of current pursuits in solid-state gas sensors. Based on the above results, we can see that the nano-Ag/In_2O_3 sensors exhibit much better gas response and lower operating temperature. Figure 8, represents the bar diagram indicating selectivity of nano-Ag surface-modified In_2O_3 sensor dipped for 30 min, and the operating temperature is 100°C to H_2S gas against the other gases. The sensor is the excellent selective to H_2S gas.

Figure 9 shows the variation of gas response with dipping time and the amount of nano-Ag (wt%). The sensor dipped for 30 min showed the maximum gas response to H_2S gas at operating temperature 100°C. At 30 min dipping time, the senor would find Ag (0.38 wt%) to be optimum. The optimum wt% of Ag (0.38) would cover the film surface uniformly. The lower gas response at higher operating temperature would be due to consumption of H_2S gas by adsorbed oxygen. At higher wt%, the Ag surfactant would mask the base material and resist the gas to reach to the surface active sites, so that gas response decreases.

5. Conclusions

The following conclusions can be drawn from the experimental results

(1) The In_2O_3 was found to be nonstoichiometric and oxygen-deficient material. It showed negative temperature coefficient in nature.
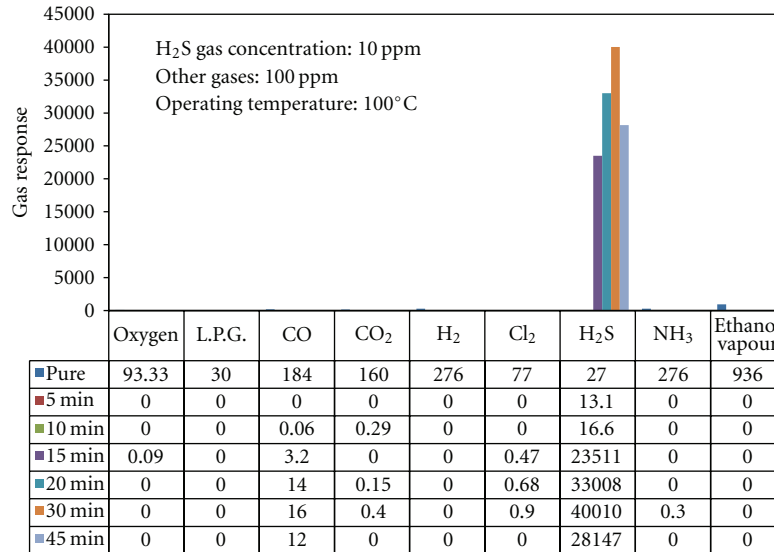
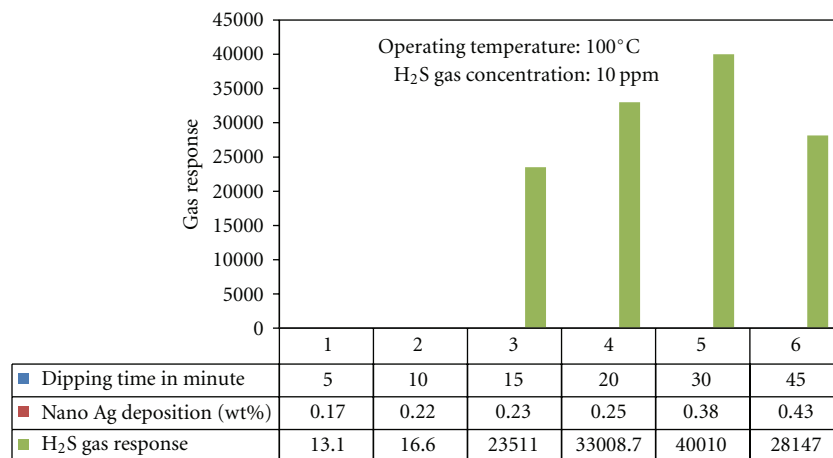FIGURE 8: Selectivity of pure and nano-Ag surface-modified In_2O_3 sensors at operating temp. 100°C.

	Oxygen	L.P.G.	CO	CO_2	H_2	Cl_2	H_2S	NH_3	Ethanol vapour
Pure	93.33	30	184	160	276	77	27	276	936
5 min	0	0	0	0	0	0	13.1	0	0
10 min	0	0	0.06	0.29	0	0	16.6	0	0
15 min	0.09	0	3.2	0	0	0.47	23511	0	0
20 min	0	0	14	0.15	0	0.68	33008	0	0
30 min	0	0	16	0.4	0	0.9	40010	0.3	0
45 min	0	0	12	0	0	0	28147	0	0

FIGURE 9: Variation of gas response with dipping time and the amount of nano-Ag (wt%).

	1	2	3	4	5	6
Dipping time in minute	5	10	15	20	30	45
Nano Ag deposition (wt%)	0.17	0.22	0.23	0.25	0.38	0.43
H_2S gas response	13.1	16.6	23511	33008.7	40010	28147

(2) The pure In_2O_3 sensor showed the highest response to ethanol vapour (80 ppm) at 350°C.

(3) The In_2O_3 sensors were modified by nano-Ag solution by dipping technique. The surface-modified sensors showed the best response to H_2S gas (10 ppm).

(4) The surface modification shifts the gas response of the sensor from ethanol vapour to H_2S gas.

(5) Since introduction of nano-Ag on the surface would alter the adsorption-desorption relationship of the sensor, the optimum dipping time was found to be 30 min.

(6) The surface modification alters only the surface morphology of the sensors not the bulk properties.

(7) The surface modification facilitated adsorption of larger number of oxygen ions on the surface could immediately oxidize the exposed H_2S gas leading to faster response time of the sensor.

(8) The surface-modified In_2O_3 sensor was observed to be excellent selective to H_2S gas.

(9) The quick response of the sensor could be attributed to larger oxygen deficiency in the surface-modified In_2O_3 sensor.

Acknowledgments

References

[1] M. Ando, S. Suto, T. Suzuki et al., "Hydrogen sulfide sensing characteristics of tin oxide sol-derived thin films," *Journal of the Ceramic Society of Japan*, vol. 104, no. 5, pp. 409–414, 1996.

[2] G. Sberveglieri, S. Groppelli, P. Nelli, C. Perego, G. Valdre, and A. Camanzi, "Detection of sub-ppm H_2S concentrations bySnO_2 (pt) thin films grown by the RGTO technique," *Sensors and Actuators B*, vol. 55, pp. 86–89, 1998.

[3] D. J. Smith, J. F. Vatelino, R. S. Falconer, and E. L. Wittman, "Stability, sensitivity and selectivity of tungsten trioxide films for sensing applications," *Sensors and Actuators B*, vol. 13, no. 1–3, pp. 264–268, 1993.

[4] H. M. Lin, C. M. Hsu, H. Y. Yang, P. Y. Lee, and C. C. Yang, "Nanocrystalline WO_3-based H_2S sensors," *Sensors and Actuators B*, vol. 22, no. 1, pp. 63–68, 1994.

[5] W. H. Tao and C. H. Tsai, "H_2S sensing properties of noble metal doped WO_3 thin film sensor fabricated by micromachining," *Sensors and Actuators B*, vol. 81, no. 2-3, pp. 237–247, 2002.

[6] J. Xu, X. Wang, and J. Shen, "Hydrothermal synthesis of In_2O_3 for detecting H_2S in air," *Sensors and Actuators B*, vol. 115, no. 2, pp. 642–646, 2006.

[7] C. Wang, X. Chu, and M. Wu, "Detection of H_2S down to ppb levels at room temperature using sensors based on ZnO nanorods," *Sensors and Actuators B*, vol. 113, no. 1, pp. 320–323, 2006.

[8] K. I. Gnanasekar, V. Jayaraman, E. Prabhu, T. Gnanasekaran, and G. Periaswami, "Electrical and sensor properties of $FeNbO_4$: a new sensor material," *Sensors and Actuators B*, vol. 55, no. 2, pp. 170–174, 1999.

[9] Y. L. Liu, H. Wang, Y. Yang et al., "Hydrogen sulfide sensing properties of $NiFe_2O_4$ nanopowder doped with noble metals," *Sensors and Actuators B*, vol. 102, no. 1, pp. 148–154, 2004.

[10] P. Siciliano, "Preparation, characterisation and applications of thin films for gas sensors prepared by cheap chemical method," *Sensors and Actuators B*, vol. 70, no. 1–3, pp. 153–164, 2000.

[11] H. Ogawa, M. Nishikawa, and A. Abe, "Hall measurement studies and an electrical conduction model of tin oxide ultrafine particle films," *Journal of Applied Physics*, vol. 53, no. 6, pp. 4448–4455, 1982.

[12] N. Yamazoe, "New approaches for improving semiconductor gas sensors," *Sensors and Actuators B*, vol. 5, no. 1–4, pp. 7–19, 1991.

[13] B. P. J. De Lacy Costello, R. J. Ewen, N. Guernion, and N. M. Ratcliffe, "Highly sensitive mixed oxide sensors for the detection of ethanol," *Sensors and Actuators B*, vol. 87, no. 1, pp. 207–210, 2002.

[14] M. Penza, C. Martucci, and G. Cassano, "NO_x gas sensing characteristics of WO_3 thin films activated by noble metals (Pd, Pt, Au) layers," *Sensors and Actuators B*, vol. 50, no. 1, pp. 52–59, 1998.

[15] G. Korotchenkov, V. Brynzari, and S. Dmitriev, "SnO_2 films for thin film gas sensor design," *Materials Science and Engineering B*, vol. 63, no. 3, pp. 195–204, 1999.

[16] A. M. Servent, D. G. Rickerby, M. C. Horrillo, R. G. Saint-Jacques, and J. Guitierrez, "Transmission electron microscopy investigation of SnO_2 thin films for sensor devices," *Nanostructured Materials*, vol. 11, pp. 813–819, 1999.

[17] S. Kaciulis, L. Pandolfi, S. Viticoli et al., "Investigation of thin films of mixed oxides for gas-sensing applications," *Surface and Interface Analysis*, vol. 34, no. 1, pp. 672–676, 2002.

[18] G. Sarala Devi, S. Manorama, and V. J. Rao, "High sensitivity and selectivity of an SnO_2 sensor to H_2S at around 100 °C," *Sensors and Actuators B*, vol. 28, no. 1, pp. 31–37, 1995.

[19] I. Jiménez, J. Arbiol, G. Dezanneau, A. Cornet, and J. R. Morante, "Crystalline structure, defects and gas sensor response to NO_2 and H_2S of tungsten trioxide nanopowders," *Sensors and Actuators B*, vol. 93, no. 1–3, pp. 475–485, 2003.

[20] B. L. Zhua, C. S. Xie, J. Wu, D. W. Zeng, A. H. Wang, and X. Z. Zhao, "Influence of Sb, In and Bi dopants on the response of ZnO thick films to VOCs," *Materials Chemistry and Physics*, vol. 96, p. 459, 2006.

[21] G. N. Chaudhari, A. M. Bende, A. B. Bodade, S. S. Patil, and V. S. Sapkal, "Structural and gas sensing properties of nanocrystalline TiO_2: WO_3-based hydrogen sensors," *Sensors and Actuators B*, vol. 115, no. 1, pp. 297–302, 2006.

[22] M. Kugishima, K. Shimanoe, and N. Yamazoe, "C_2H_4O sensing properties for thick film sensor using La_2O_3-modified SnO_2," *Sensors and Actuators B*, vol. 118, no. 1-2, pp. 171–176, 2006.

[23] C. S. Rout, A. R. Raju, A. Govindaraj, and C. N. R. Rao, "Hydrogen sensors based on ZnO nanoparticles," *Solid State Communications*, vol. 138, no. 3, pp. 136–138, 2006.

[24] W. Gopel and K. D. Schierbaum, "SnO sensors: Current status and future prospects," *Sensors and Actuators B*, vol. 26–27, pp. 1–12, 1995.

[25] D. M. Wilson, K. Dunman, T. Roppel, and R. Kalim, "Rank extraction in tin-oxide sensor arrays," *Sensors and Actuators B*, vol. 62, no. 3, pp. 199–210, 2000.

[26] M. S. Dutraive, R. Lalauze, and C. Pijolat, "Sintering catalytic effects and defect chemistry in polycrystalline tin dioxide," *Sensors and Actuators B*, vol. 26, no. 1–3, pp. 38–44, 1995.

[27] M. Gaidi, B. Chenevier, and M. Labeau, "Electrical properties evolution under reducing gaseous mixtures (H_2, H_2S, CO) of SnO_2 thin films doped with Pd/Pt aggregates and used as polluting gas sensors," *Sensors and Actuators B*, vol. 62, no. 1, pp. 43–48, 2000.

[28] K. Wada and M. Egashira, "Hydrogen sensing properties of SnO_2 subjected to surface chemical modification with ethoxysilanes Sens," *Sensors and Actuators B*, vol. 62, p. 211, 2000.

[29] G. Faglia, B. Allieri, E. Comini, L. E. Depero, L. Sangaletti, and G. Sberveglieri, "Electrical and structural properties of RGTO-In_2O_3 sensors for ozone detection," *Sensors and Actuators B*, vol. 57, no. 1–3, pp. 188–191, 1999.

[30] H. Steffes, C. Imawan, F. Solzbacher, and E. Obermeier, "Fabrication parameters and NO_2 sensitivity of reactively RF-sputtered In_2O_3 thin films," *Sensors and Actuators B*, vol. 68, no. 1, pp. 249–253, 2000.

[31] T. V. Belysheva, E. A. Kazachkov, and E. E. Gutman, "Gas sensing properties of In_2O_3 and Au-doped In_2O_3 films for detecting carbon monoxide in air," *Journal of Analytical Chemistry*, vol. 56, no. 7, pp. 759–762, 2001.

[32] J. R. Bellingham, A. P. Mackenzie, and W. A. Phillips, "Precise measurements of oxygen content: oxygen vacancies in transparent conducting indium oxide films," *Applied Physics Letters*, vol. 58, no. 22, pp. 2506–2508, 1991.

[33] M. Law, H. Kind, B. Messer, F. Kim, and P. Yang, "Photochemical sensing of NO_2 with SnO_2 nanoribbon nanosensors at room temperature," *Angewandte Chemie—International Edition*, vol. 41, no. 13, pp. 2405–2408, 2002.

[34] A. Kolmakov, Y. Zhang, G. Cheng, and M. Moskovits, "Detection of CO and O_2 using tin oxide nanowire sensors," *Advanced Materials*, vol. 15, no. 12, pp. 997–1000, 2003.

[35] N. Koshizaki and T. Oyama, "Sensing characteristics of ZnO-based NO_x sensor," *Sensors and Actuators B*, vol. 66, no. 1, pp. 119–121, 2000.

[36] G. S. T. Rao and D. Tarakarama Rao, "Gas sensitivity of ZnO based thick film sensor to NH_3 at room temperature," *Sensors and Actuators B*, vol. 55, no. 2, pp. 166–169, 1999.

[37] C. Li, D. Zhang, X. Liu et al., "In$_2$O$_3$ nanowires as chemical sensors," *Applied Physics Letters*, vol. 82, no. 10, pp. 1613–1615, 2003.

[38] G. Korotechnov, V. Brynzari, and S. Dmitriev, "SnO$_2$ film for thin film gas sensor design," *Materials Science and Engineering*, vol. 56, pp. 195–204, 1999.

[39] A. M. Servent, D. G. Rickerby, M. C. Horrillo, R. G. Saint-Jacques, and J. Guitierrez, "Transmission electron microscopy investigation of SnO$_2$ thin films for sensor devices," *Nanostructured Materials*, vol. 11, pp. 813–819, 1999.

[40] S. Kaciulis, L. Pandolfi, S. Viticoli et al., "Investigation of thin films of mixed oxides for gas-sensing applications," *Surface and Interface Analysis*, vol. 34, no. 1, pp. 672–676, 2002.

[41] P. K. Khanna, N. Singh, D. Kulkarni, S. Deshmukh, S. Charan, and P. V. Adhyapak, "Water based simple synthesis of re-dispersible silver nano-particles," *Materials Letters*, vol. 61, no. 16, pp. 3366–3370, 2007.

[42] K. D. Schierbaum, U. K. Kirner, J. F. Geiger, and W. Göpel, "Schottky-barrier and conductivity gas sensors based upon Pd/SnO$_2$ and Pt/TiO$_2$," *Sensors and Actuators B*, vol. 4, no. 1-2, pp. 87–94, 1991.

[43] G. H. Jain, V. B. Gaikwad, D. D. Kajale et al., "Gas sensing performance of pure and modified BST thick film resistor," *Sensors and Transducers*, vol. 90, pp. 160–173, 2008.

[44] S. M. A. Durrani, E. E. Khawaja, and M. F. Al-Kuhaili, "CO-sensing properties of undoped and doped tin oxide thin films prepared by electron beam evaporation," *Talanta*, vol. 65, no. 5, pp. 1162–1167, 2005.

[45] G. H. Jain, L. A. Patil, and V. B. Gaikwad, "Studies on gas sensing performance of $(Ba_{0.8}Sr_{0.2})(Sn_{0.8}Ti_{0.2})O_3$ thick film resistors," *Sensors and Actuators B*, vol. 122, no. 2, pp. 605–612, 2007.

[46] V. D. Kapse, S. A. Ghosh, G. N. Chaudhari, F. C. Raghuwanshi, and D. D. Gulwade, "H$_2$S sensing properties of La-doped nanocrystalline In$_2$O$_3$," *Vacuum*, vol. 83, no. 2, pp. 346–352, 2008.

[47] G. H. Jain, L. A. Patil, M. S. Wagh, D. R. Patil, S. A. Patil, and D. P. Amalnerkar, "Surface modified BaTiO$_3$ thick film resistors as H$_2$S gas sensors," *Sensors and Actuators B*, vol. 117, no. 1, pp. 159–165, 2006.

[48] N. Iftimie, E. Rezlescu, P. D. Popa, and N. Rezlescu, "Gas sensitivity of nanocrystalline nickel ferrite," *Journal of Optoelectronics and Advanced Materials*, vol. 8, no. 3, pp. 1016–1018, 2006.

[49] G. Xu, Y. W. Zhang, X. Sun, C. L. Xu, and C. H. Yan, "Synthesis, structure, texture, and CO sensing behavior of nanocrystalline tin oxide doped with scandia," *Journal of Physical Chemistry B*, vol. 109, no. 8, pp. 3269–3278, 2005.

[50] S. R. Morrison, "Mechanism of semiconductor gas sensor operation," *Sensors and Actuators*, vol. 11, no. 3, pp. 283–287, 1987.

[51] P. K. Khanna, N. Singh, D. Kulkarni et al., "One-step preparation of nanosized Ag-Pd co-powder and its alloy formation at low temperature," *Synthesis and Reactivity in Inorganic, Metal-Organic and Nano-Metal Chemistry*, vol. 37, no. 7, pp. 531–539, 2007.

[52] D. R. Patil and L. A. Patil, "Cr$_2$O$_3$-modified ZnO thick film resistors as LPG sensors," *Talanta*, vol. 77, no. 4, pp. 1409–1414, 2009.

[53] C. Xiangfeng, J. Dongli, G. Yu, and Z. Chenmou, "Ethanol gas sensor based on CoFe$_2$O$_4$ nano-crystallines prepared by hydrothermal method," *Sensors and Actuators B*, vol. 120, no. 1, pp. 177–181, 2006.

[54] Y. L. Liu, H. Wang, Z. M. Liu, H. F. Yang, G. L. Shen, and R. Q. Yu, "Hydrogen Sulfied sensing properties of NiFeO$_4$ nanopowder doped with nobel metal," *Sensors & Actuators B*, vol. 102, pp. 148–154, 2004.